



available at www.sciencedirect.com



journal homepage: www.elsevier.com/locate/jhydrol



Spatial and temporal variability of soil saturated hydraulic conductivity in gradients of disturbance

Beate Zimmermann ^{a,*}, Helmut Elsenbeer ^b

^a *Smithsonian Tropical Research Institute, Balboa, Panama*

^b *Institute of Geoecology, University of Potsdam, 14476 Potsdam, Germany*

Received 30 November 2007; received in revised form 26 June 2008; accepted 17 July 2008

KEYWORDS

Soil hydrology;
Saturated hydraulic
conductivity;
Tropical montane
rainforest;
Disturbance and
recovery;
Landslides;
Land use

Summary Tropical montane rain forests are subject to both natural and anthropogenic disturbances, such as shallow landslides and forest-to-pasture conversion. Vegetation regrowth is rapid upon attaining hillslope stability and pasture abandonment, respectively, and apt to affect soil hydrology via changes in soil structure, a sensitive indicator of which is soil saturated hydraulic conductivity (K_s). Our objective was to quantify the influence of these regionally widespread and important disturbances on K_s and the subsequent recovery of K_s , and to describe the resulting spatial patterns.

In a 2 km² large research area in southern Ecuador, we used a mixed design- and model-based sampling strategy for measuring K_s in situ at soil depths of 12.5, 20, and 50 cm ($n = 30\text{--}150/\text{depth}$) under landslides of different ages (2 and 8 years), under actively grazed pasture, fallows following pasture abandonment (2–25 years of age), and under natural forest, and for elucidating its spatial patterns.

Global means of soil permeability generally decrease with increasing soil depth. K_s does not differ among landslides and in comparison to the natural forest, which suggests a marginal effect of the regional landslide activity on soil hydrology. In contrast, results from the human-induced disturbance regime show a permeability decrease of two orders of magnitude after forest conversion to pasture at shallow soil depths, and a slow regeneration after pasture abandonment that requires a recovery time of at least one decade.

Disturbances affect the K_s spatial structure, in particular the correlation length, in the topsoil. The largest differences in the covariance parameters, however, are found for the subsoil K_s , where the spatial structure is independent of land cover.

This case study suggests a rather disparate soil hydraulic response to regionally important disturbances. Cattle grazing strongly affects the spatial mean of K_s , whereas landslides do not, and both the processes affect the spatial structure of K_s in the topsoil.

© 2008 Elsevier B.V. All rights reserved.

* Corresponding author. Formerly at Institute of Geoecology, University of Potsdam, 14476 Potsdam, Germany. Tel.: +507 2128295.
E-mail address: ZimmermannB@si.edu (B. Zimmermann).

Introduction

Disturbances are part of natural ecosystems dynamics. In forested regions, ecosystem-inherent disturbances include treefall, outbreak of herbivores, fires, floods, and mass movements, which take place over a wide range of spatial and temporal scales. Some disturbances do merely destroy the vegetation itself, whereas others potentially impact abiotic components of the ecosystem. Landslides belong to the latter as they are initiated in the soil body and in return affect soil properties.

In humid tropical environments characterized by steep slopes, high rainfall, and frequent catastrophic events such as hurricanes or earthquakes, landslides are a common phenomenon (Terlien, 1997; Larsen et al., 1999; Vieira and Fernandes, 2004). In montane rainforests of the south Ecuadorian Andes, they are an intrinsic part of the natural disturbance regime. Because of their potentially devastating consequences for human life and local economies, the management of landslide risks and the prediction of landslide hazards have received considerable attention (e.g. Terlien, 1997; Zaitchik et al., 2003; Brenning, 2005). The few studies that dealt with the impact of landslide disturbance and recovery on soil properties in pristine ecosystems focused on soil fertility and soil organic matter (e.g. Walker et al., 1996; Singh et al., 2001; Wilcke et al., 2003). Larsen et al. (1999) and Hou et al. (2005) studied erosion processes and soil fauna, respectively, under undisturbed forest and on recent landslide scars. Regarding soil hydrology, Vieira and Fernandes (2004) investigated the saturated hydraulic conductivity on and next to landslide scars near Rio de Janeiro. To our knowledge, however, no study has yet attempted to quantify the soil hydraulic response to landsliding in tropical montane rainforests, though landslides figure prominently in this environment.

In addition to this ecosystem-inherent disturbance, forest conversion for pasture establishment has become a cause of disturbance in this region over the past 60 years. This development is a cause of concern, because tropical montane rainforests are the most endangered of tropical forest ecosystems, with an annual rate of deforestation of about 1.1% for 1981–1990, which is greater than the overall rate of deforestation in the tropics (Bruijnzeel, 2001). In the montane rainforest of south Ecuador, deforestation initiates a 'vicious circle' (Hartig and Beck, 2003).

After repeated burning of the natural forest, pasture grasses or short-term crops (beans and maize), which may precede pasture establishment, and bracken (*Pteridium arachnoideum*) develop simultaneously. Due to the widespread practice of frequently burning bracken-invaded pastures, the cycle of the concurrent bracken and pasture development is repeated several times. The increasing density of fern rhizomes, combined with an ongoing weakening of the grass tussocks, reduces the period of improved grass growth with every fire. After less than 10 years on average, bracken takes over completely and pastures are abandoned. The final succession stage consists of patches of bracken separated by 2–3 m – high bushes. The high potential of bushes and bracken to propagate from seeds and rhizomes, respectively, appears to ensure a high stability of this vegetative type and a long-lasting serial stage. Natural forest recovery is unlikely mainly because of restricted seed dispersal.

These human and natural disturbance characteristics of our montane rainforest study site are summarized in Fig. 1.

Soil degradation processes may also influence the natural succession (Guenther et al., 2006). Little is yet known, however, about the influence of land use and subsequent recovery on soil hydraulic properties in tropical mountainous regions. An exception is Ziegler et al. (2004), who studied changes in the soil hydrological behavior due to land use in a tropical mountainous rainforest region in Vietnam. The influence of pasture establishment and subsequent fallows on soil hydrology is still poorly known despite the broad extension of those land covers in tropical montane rainforest environments.

To our knowledge, no study of saturated hydraulic conductivity yet exists that attempted to estimate the spatial covariance parameters as a function of land use or disturbance. In the humid tropics, Sobieraj et al. (2004) investigated the K_s spatial structure in soils under primary rainforest; a number of studies dealt with K_s spatial variability of agricultural soils in the temperate regions (e.g. Mohanty et al., 1991; Reynolds and Zebchuk, 1996; Bosch and West, 1998; Mohanty and Mousli, 2000; Shukla et al., 2004).

Our long-term objective is to quantify the influence of natural and man-made disturbances and the subsequent recovery on a key property of the hydrologic cycle – the soil saturated hydraulic conductivity – and to describe the resulting spatial–temporal pattern. We selected the saturated hydraulic conductivity (K_s from here on) because it has shown to be a sensitive indicator of soil disturbances (Ziegler et al., 2004; Zimmermann et al., 2006). The objective of this case study was to address these research questions:

- (1) Do the prevalent natural and man-made disturbances in the montane rainforest cause an apparent displacement of the less permeable soil layer towards the surface, either due to a loss of the permeable surface soil after land-sliding, or as a consequence of the surface soil compaction under cattle pastures?
- (2) Does 'recovery' from disturbance, either because of landslide re-vegetation or because of secondary succession after pasture abandonment, involve an apparent displacement of the less permeable layer back towards the original depth?

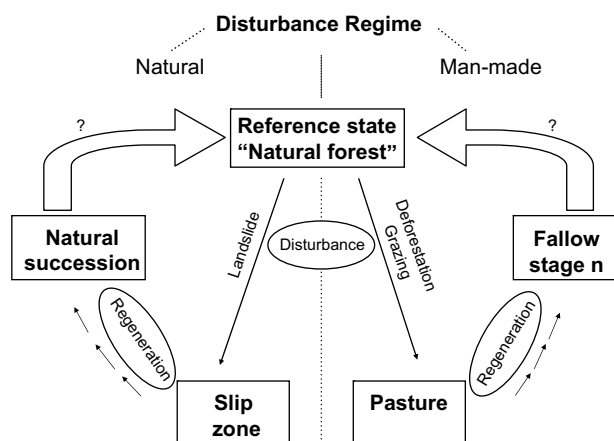


Figure 1 Conceptual framework of the study.

- (3) Do disturbances cause a simplification of the K_s spatial structure, and does the subsequent recovery entail the re-establishment of the original structure?

Materials and methods

Study area

Embedded in the Eastern Cordillera of the Andes of southern Ecuador, our study area (Fig. 2) is located in the Reserva Biósfera de San Francisco around the Estación Científica San Francisco (ECSF) ($3^{\circ}58'18''$ S, $79^{\circ}4'45''$ W, 1860 m a.s.l.). Steep slopes ($30\text{--}50^{\circ}$) covered by “Lower Montane Rain Forest”, which gradually changes to “Lower Montane Cloud Forest” on higher ground (Bruijnzeel and Hamilton, 2000), characterize the north-facing valley side of the Rio San Francisco, where recent human intervention is virtually absent. By contrast, the south-facing valley side has been subject to human influence for decades. Shallow translational landslides are frequent throughout the study region, where 3.7% of an 1117-ha forested study area was covered by visible landslides in 1998 (Wilcke et al., 2003). We observed minor recent slip activity at pastures and on fallows potentially due to the absence of forest biomass, which is

assumed to be of major importance for landslide initiation in this area.

Mean annual precipitation (1998–2005) amounted to 2273 mm (Rollenbeck et al., 2007) and mean annual (1999–2002) air temperature was 15.5°C (Motzer et al., 2005). A drier period is between November and January & May and June are the wettest months (Motzer et al., 2005).

The bedrock consists mainly of weakly metamorphosed Palaeozoic schists and sandstones with some quartz veins (Wilcke et al., 2003), which belong to the Chiguinda unit (Mapa geológico del Ecuador; Instituto Geográfico de Militar y Ministerio de Energía y Minas). Soils are classified as Inceptisols and Histosols (Soil Survey Staff, 1999; Schrumpp et al., 2001) with a high percentage of silt.

Site selection

We selected four plots that represent the human disturbance and recovery sequence, and two landslides of increasing age. All plots are free of micro-topographic peculiarities such as big hollows, rills or gullies; slopes amounted to 30° till 40° , and aspects were similar. Both chronosequences have their old-growth forest reference since they are located on the two opposite valley sides (Fig. 2). Hence, initial conditions may differ due to their distinct landscape

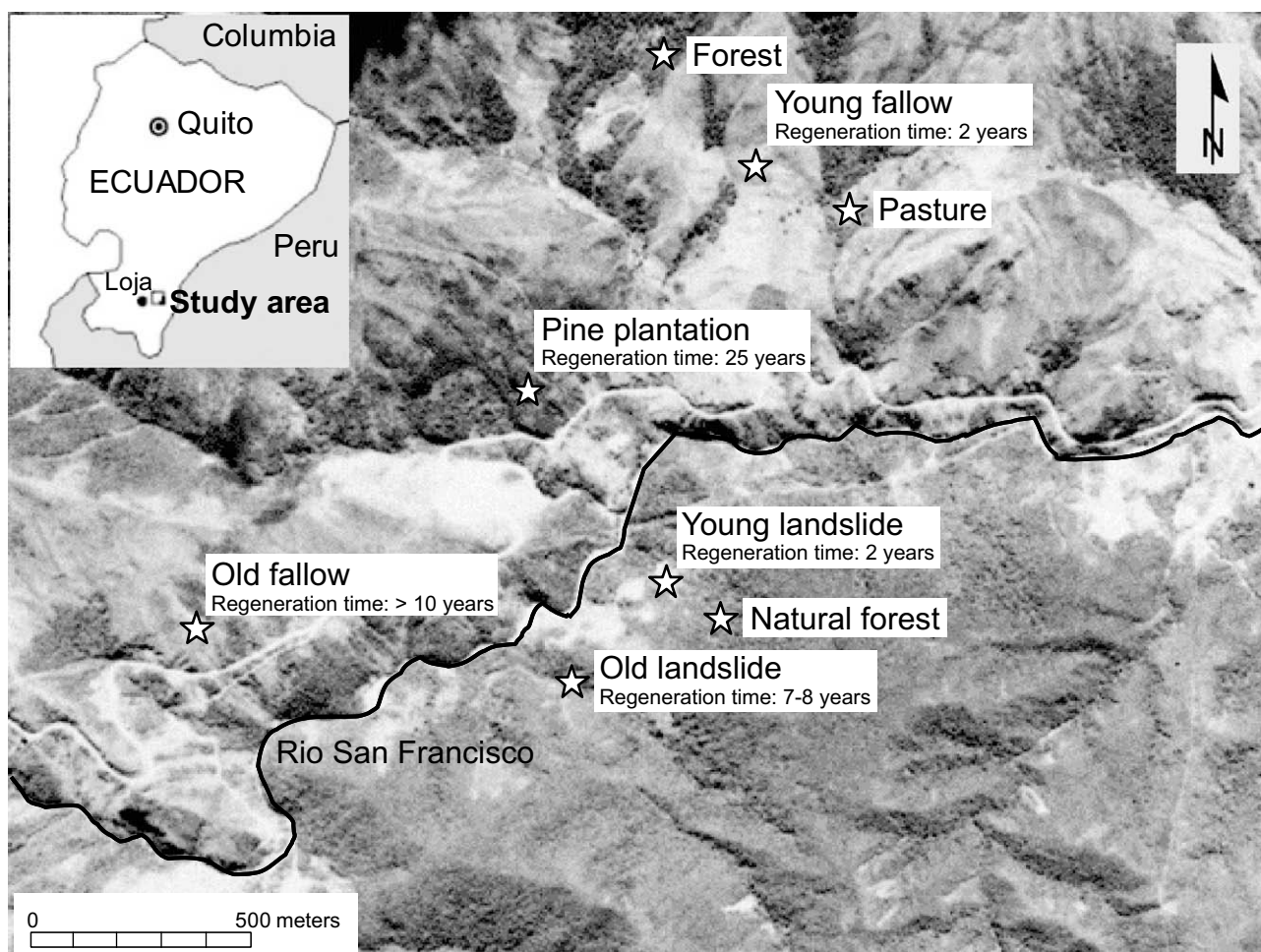


Figure 2 Map and aerial view of the research area. Plot locations are indicated by asterisks.

history associated with e.g. higher frequencies of fires and the rareness of landslides in the areas influenced by human activities.

The reference site for the natural disturbance cycle is covered by "Lower Montane Rain Forest" (Bruijnzeel and Hamilton, 2000), underlain by a Humic Dystrudept (Goller et al., 2005) with a silt content of about 60% in all horizons (Schrumpf et al., 2001).

The young landslide (YS) occurred two years before our measurement campaign about 200 m to the northwest of the reference site. This slide consists of clearly distinguishable zones: below the scar is the slip zone, the zone of interest for the purposes of this study. This is followed downwards by a very steep and narrow depletion zone. At this position, a recently formed gully extends down to the accumulation zone at the foot of the landslide. Any successional vegetation is restricted to the accumulation zone.

An older landslide (OS) is located in an adjacent catchment and was active about 7–8 years ago. Successional plants include mosses, grasses, bracken, and small shrubs, but also bigger shrubs and small trees that occur on "accumulation islands"; only the former slip zone is still bare of vegetation. This landslide is part of the landslide chronosequence, whose soil properties were studied by Wilcke et al. (2003).

The reference forest (FO) on the south-facing valley side for the human disturbance cycle shows signs of interference, such as logs of cut trees and charcoal in the upper soil. Two soil profiles illustrated the high variability over very short distances: one showed an initial stage of soil development with an A-horizon overlying the parent material, whereas the other a well-defined B-horizon had already developed. At some measurement locations, a buried organic layer in about half a meter soil depth indicates former slide activities.

Our pasture plot (PA) has been grazed for about 20 years. Numerous narrow cattle trails are distributed along the contour lines. The dominant grass species are *Setaria sphacelata* on less inclined slope portions and *Melinis minutiflora* on steeper slopes. The low palatability of *Setaria* and the low biomass production of *Melinis* explain the low carrying capacity in the study region (Hartig and Beck, 2003).

The young fallow (YF) was abandoned from pasture use only two years before our measurements, which accounts for the rather unusual dominance of *Setaria* instead of bracken.

After a recovery of at least 10 years, succession vegetation covers the old fallow (OF), but bracken is still frequent.

Among the most abundant families are *Orchidaceae*, *Asteraceae*, *Ericaceae*, *Melastomataceae*, *Poaceae*, *Rosaceae*, *Gleicheniaceae*, *Lycopodiaceae*, *Bromeliaceae*, and *Myrsinaceae*, which are the same pioneers as on the landslides.

The pine plantation (PI) represents a special type of a secondary forest; pines (*Pinus patula*) were planted immediately after pasture abandonment 25 years ago. The space between the sparsely standing trees is almost completely covered by bracken, which in places grows taller than 2 m.

Table 1 provides a summary of all plot descriptions and abbreviations of the plot names, which will be used in the text from here on.

Field measurements of saturated hydraulic conductivity

We measured the saturated hydraulic conductivity in situ in the mineral soil at the depths of 12.5, 20 and 50 cm with an Amoozometer (Ksat Inc., Raleigh; Amoozegar, 1989a,b; Amoozegar, 1993), a compact, constant-head permeameter. The procedure involved augering a cylindrical hole with radius r to the desired depth, establishing a constant head H such that $H/r \geq 5$, and monitoring the outflow from the device until a steady-state flow rate is attained; at which point K_s can be calculated via the Glover solution (Amoozegar, 1989b). This model deals only with one equation, based on gravitational flow and gravitational potential (Amoozegar, 1993). For a comparison of calculated K_s by the Glover equation with the calculated K_s using different Alpha parameter values (Erick and Reynolds, 1992), the Glover equation gave results that were comparable to the results obtained by the fixed Alpha value approach (Amoozegar, personal communication).

For all land covers except the young landslide, the pine plantation, and the forest at the land-use site, we used a combined design- and model-based sampling approach to satisfy the preconditions both for inter-site comparisons and for the intra-site spatial analysis. First, we chose the location of the measurement plot such that its x-axis corresponded to a contour line of the investigated hillslope (Fig. 3); in the case of the old landslide, feature and plot overlapped completely. We then superimposed a grid consisting of grid cells of a size of 2 m²; a total of 30 grid cells was then included in our sample using a random selection algorithm. Within each selected cell we placed five fixed measuring points (Fig. 3). The spacing among those points was based upon experience from a former study in the Brazilian Amazon, where spatial patterns of K_s emerged only at

Table 1 Selected site properties

Land cover type	Abbreviation	Altitude (m a.s.l.)	Average slope (°)	Aspect	Sampled area/plot (ha)	Recovery time (years)
Young landslide	YS	2000	35	W	– (Slip zone)	2
Old landslide	OS	1900	35	S	0.06 (Entire slide)	7–8
Natural forest	NF	2000	35	NW	0.4	–
Pasture	PA	2000	35	SW	0.5	0
Young fallow	YF	2100	35	SW	0.4	2
Old fallow	OF	2100	30	SE	0.35	~10
Pine plantation	PI	1900	35	S	0.1	~25
Forest	FO	2200	35	SW	0.1	–

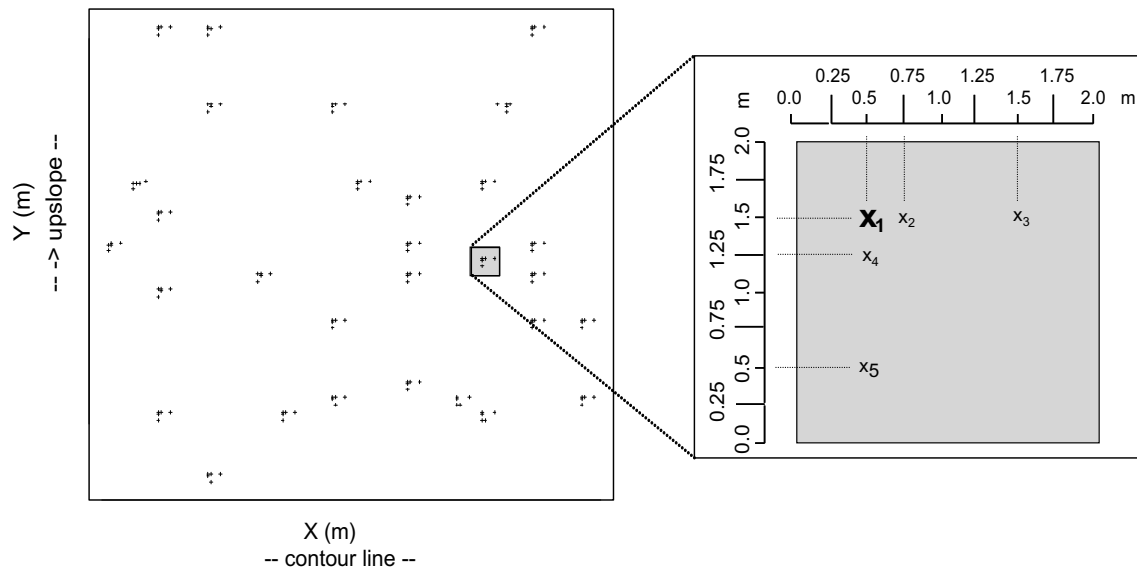


Figure 3 Sampling grid; x_1 is the sampling point used for the global comparisons.

a high sampling resolution, i.e. short lag distances (Sobieraj et al., 2004). Hence, we emphasized small separation distances, starting with the smallest possible point distance of 0.25 m (Fig. 3). This distance emerged from field trials which showed that yet smaller distances would cause prior measurements to interfere with subsequent ones.

The described procedure resulted in an irregular sampling scheme with a sample size of 150 per soil depth for the spatial analysis, which corresponds to the recommended sample size to estimate method-of-moments variograms (Webster and Oliver, 1992), and somewhat less at 50 cm depth, where augering was not possible in all places due to a large percentage of stones. Since only the selection of the squares was design-based, we used only their first point for the inter-site comparisons, which resulted in a sample size of 30 per land cover and soil depth.

For the pine plantation and the forest we took 30 sampling points via simple random sampling. At the young landslide, we measured K_s exclusively in the slip zone at 30 randomly selected locations. Measurements in the depletion zone were impossible because of its steepness, and we assume K_s under the accumulation zone to remain unchanged compared to the original state. Hence, the natural disturbance sequence exclusively compares K_s between the soils of a natural forest and an older landslide, and K_s among the forest soil and the slip zones of two landslides of different recovery times.

Statistical and geostatistical analyses

For all data analysis we used the language and environment of *R*, version 2.2.1 (R Development Core Team, 2004); many of the geostatistical methods were implemented in the libraries *geoR* (Ribeiro and Diggle, 2001) and *gstat* (Pebesma, 2004).

Initial conditions

A prerequisite for inter-site comparisons is the equality of initial conditions to ensure that the measured effects are so-

lely a consequence of the “treatment”. Since K_s is a function of the soil’s macro-porosity (Carman, 1956; Ahuja et al., 1984), it is subject to all influences that change the macro-porosity. Apart from disturbance effects, macro-porosity may vary depending on soil texture, and, particularly in the topsoil, on soil structure. Soil texture of human-disturbed plots is comparable, i.e. the soils have a high silt content, between 20% and 35% sand, and a low clay content (Fig. 4). Within the forested part of our study area, particle size distributions of the loamy soils are heterogeneous at a small scale due to the prevalent gravitational mass movements. For example, for 36 profiles in a 2500 m² plot in the forest catchment where our natural forest plot is located (Muñoz, 2005), the coefficient of variation amounts to 25% for all particle sizes; this is in the same range as the particle size variations between the intermediate slide and another one far away from the former (data from Wilcke et al., 2003). Hence, particle size distributions are more scattered for the naturally disturbed plots (Fig. 4). The soil of the intermediate slide has a sand content of more than 50% in contrast to the natural forest, where sand amounts to less than 20% of the fine-earth fraction.

Macrostructure is subangular to angular in soil profiles at both the valley sides. Regarding microstructure, the absence of swelling clays and of crystalline oxides, especially in the topsoils (Schrumpp et al., 2001), do not promote a strong influence of structural pore space (Ringrose-Voase, 1991) on the saturated hydraulic conductivity. Non-structural porosity, i.e. biopores, depends on extrinsic factors; hence, variation in soil structure can be attributed to vegetation and the corresponding edaphon. The same applies to carbon contents (Makeschin et al., 2008).

Within a given land cover, K_s may depend on topography (Huwe et al., 2008); therefore, we based our plot selection on similar slopes and slope positions (Table 1).

To avoid spatial pseudoreplication, we chose the greatest possible plot size, which ranged from 0.35 to 0.5 ha for the plots with 150 measuring points, and which covered 0.1 ha for the less intensively investigated land covers

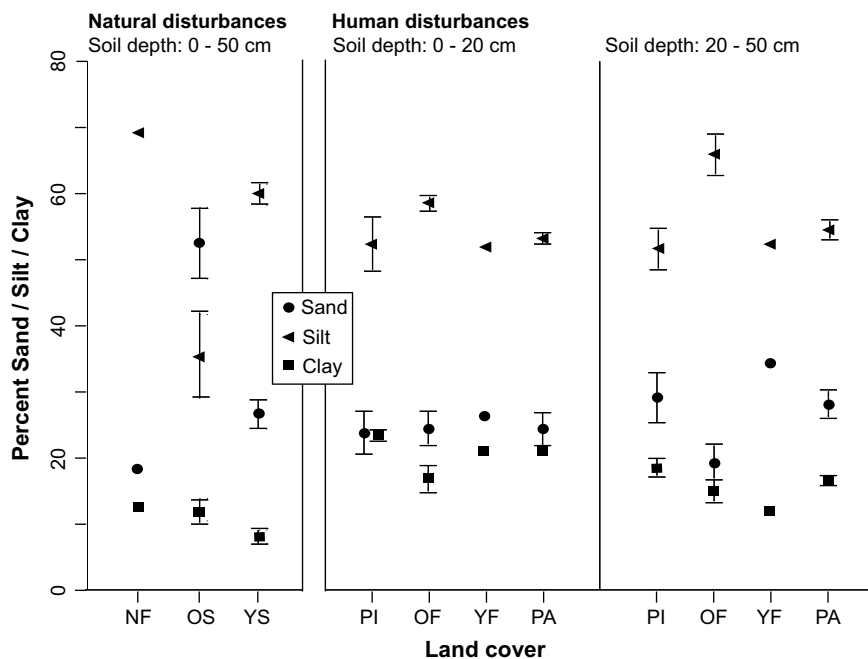


Figure 4 Mean particle size distributions (data from Wilcke et al., 2003; Makeschin, unpublished data; Huwe, unpublished data) for the investigated land covers. Bars represent the mean \pm standard errors when data of more than one profile was available. Profiles were located within the plots (PA, YF, OF, YS, OS, NF) or adjacent to the plots (PI).

(Table 1). Sampling of more than one plot per land cover was impossible due to the overall restricted accessibility and the precondition of similar slopes.

Exploratory data analysis

Since diagnostic plots indicated non-Gaussian behavior of the K_s distributions, we used Box–Cox Transformation (Box and Cox, 1964) to find the most appropriate transformation. We then checked the univariate distribution of the (transformed) data, both for the global comparison datasets and for the spatial datasets. The latter were also checked for bivariate Gaussian distributions and outliers by means of h -scattergrams (Webster and Oliver, 2001), which are scatterplots of point pairs separated by a fixed distance. We computed the Spearman rank correlation coefficient for the point pairs to get a first idea of the strength and the range of the spatial autocorrelations.

We used diagnostic plots (dividing the data into quintiles; plots of the data versus the coordinates) to explore the spatial data for non-stationarity that may be caused by local trends following the relation:

$$z(\mathbf{x}) = \mu(\mathbf{x}) + \varepsilon(\mathbf{x}), \quad (1)$$

where $z(\mathbf{x})$ is the observed variable at location \mathbf{x} , $\mu(\mathbf{x})$ is a measure of central tendency, i.e. a deterministic drift of the variable at location \mathbf{x} , and $\varepsilon(\mathbf{x})$ is the random component at location \mathbf{x} that should be normally distributed with zero mean and that satisfies the second-order stationarity required for spatial analysis. Hence, we calculated the residual values $\varepsilon(\mathbf{x})$ at every location \mathbf{x} and used the F -test (Fisher, 1972) to explore if $\mu(\mathbf{x})$ is significantly different from 0. In case of a significant deterministic trend, we estimated the trend coefficients as fixed effects by restricted maximum likelihood (see below).

Global comparisons

We used the median as a resistant estimator of location with its 95% ($\alpha = 0.05$) confidence interval calculated as follows:

$$M \pm t_{n-1} * d_F / (1.075 * n^{1/2}), \quad (2)$$

where t is the t -statistic at the 95% confidence level for a given sample size, n and d_F is the fourth spread (Iglewicz, 1983). Based on the confidence intervals, we evaluated the differences between the land covers within the human and the natural disturbance sequence, respectively. In addition, we visually classified the different zones of the older landslide as the former slip and the non-active zone, and compared their soil permeability. To allow comparability between the young and the old landslide, we used only K_s measurements of the old landslide's slip zone for the global comparison ($n = 28$ for the soil depths of 12.5 and 20 cm and $n = 14$ for the 50 cm soil depth).

Spatial analysis

As the first step in the variogram analysis, we calculated experimental variograms using the variogram estimator according to Matheron (1962):

$$2\hat{\gamma}(h) = \frac{1}{N(h)} \sum_{i=1}^{N(h)} \{z(x_i) - z(x_i + h)\}^2; \quad (3)$$

where $z(x_i)$ is the observed value at location x_i , $N(h)$ are the pairs of observations that are separated by lag h .

We next decided if we need robust estimation techniques. For this purpose, we fitted three standard theoretical variogram models (exponential, Gaussian, spherical) by ordinary least squares to the experimental variograms; the "best" model was chosen by the minimum sum of squares from the fit. We then adopted the approach of Lark

(2000), who compared the variograms derived from the Matheron estimator and three robust estimators by cross-validation or with a validation subset using a statistics $\theta(\mathbf{x})$ defined as

$$\theta(\mathbf{x}) = \frac{\{z(\mathbf{x}) - Z(\mathbf{x})\}^2}{\sigma_{k,x}^2}, \quad (4)$$

where $z(\mathbf{x})$ is the observed variable at location \mathbf{x} , $Z(\mathbf{x})$ is the kriged estimate and $\sigma_{k,x}^2$ is the kriging variance. Lark (2000) showed that $E(\text{median } \theta(\mathbf{x}))$ is 0.455 when a correct variogram is used to interpolate intrinsic data. In order to compute confidence limits for the median of $\theta(\mathbf{x})$, Lark (2000) quoted standard texts for the distribution of the sample median of a large sample of $2n + 1$ data, which are random variables of median \tilde{y} and probability density function $f(\tilde{y})$; hence, \tilde{y} is a normally distributed variable drawn from a population with variance $\sigma_{\tilde{y}}^2$, where

$$\sigma_{\tilde{y}}^2 = \frac{1}{8n * f(\tilde{y})^2}. \quad (5)$$

In the framework of the statistic $\theta(\mathbf{x})$, $f(\tilde{y})$ is the pdf of the χ^2 distribution with 1 df, the median of which is 0.455.

At this point, the confidence limits can be computed by

$$0.455 \pm 1.96 * \sqrt{\sigma_{\tilde{y}}^2}. \quad (6)$$

If the median of $\theta(\mathbf{x})$ indicates that Matheron's estimator is significantly influenced by outliers, robust estimation techniques should be used.

We also checked our data for anisotropy by calculating the experimental variograms in four different directions, one representing the contour line, one the slope and the other two are in between those two extremes.

If the median of $\theta(\mathbf{x})$ ruled out the presence of influential extreme values we estimated the covariance parameters nugget, sill, and range by restricted maximum likelihood as proposed by Lark et al. (2006). The principle of maximum likelihood estimation of variogram parameters is as follows: n observed data are assumed to be from a multivariate Gaussian distribution with a mean vector \mathbf{m} of length n and a covariance matrix Σ ; the joint probability density of the data is

$$g(\mathbf{z}) = (2\pi)^{-n/2} |\Sigma|^{-1/2} \exp \left\{ -\frac{1}{2} (\mathbf{z} - \mathbf{m})^T \Sigma^{-1} (\mathbf{z} - \mathbf{m}) \right\}. \quad (7)$$

The vector \mathbf{z} contains the n data and the vector \mathbf{p} contains the parameter of the covariance matrix Σ . If the mean \mathbf{m} and the covariance Σ are unknown and depend on parameter vectors \mathbf{m} and \mathbf{p} , respectively, one can regard \mathbf{z} as fixed and $g(\mathbf{z})$ as a function of \mathbf{m} and \mathbf{p} , which is called the likelihood function $L(\mathbf{m}, \mathbf{p})$. Maximizing the likelihood, or minimizing the negative log-likelihood $-\log L(\mathbf{m}, \mathbf{p})$ yields the parameter estimates. If a trend is apparent, the joint determination of the trend and the covariance parameters are prone to bias. The solution to this problem is to use restricted maximum likelihood (REML) to estimate the variance parameters, because it removes the dependence of the estimates on the nuisance parameter \mathbf{m} . Next, a mixed modeling procedure is used to estimate the fixed effects (e.g. the coefficients of a trend model), the random effects (the spatially dependent random variation), and the random

error (nugget variation). For a detailed mathematical description of the method we refer to Lark et al. (2006). We again used the three standard model types, because we could not fit the more flexible Matérn model (Whittle, 1954; Matérn, 1960) for a number of datasets. This impossibility was due to flat likelihood functions, when we estimated the additional smoothness parameter of the Matérn function.

Estimation by REML requires a multivariate Gaussian distribution, which cannot be verified (Pardo-Igúzquiza, 1998), which is why we scrutinized the h-scattergrams to at least check for bivariate Gaussian distributions. To rule out distortion of the REML-estimated covariance parameters due to skewness, we compared them with those of the least-squares models of the Matheron experimental variogram.

In order to compare the covariance parameters between the land covers, we calculated the effective range to allow for comparability of the correlation lengths independent of the model type. The effective range for the spherical model coincides with the model range; for the exponential model, the effective range is approximately the model range times 3, and for the Gaussian model it is estimated by the model range times the square root of 3 (Webster and Oliver, 2001).

We also wanted to compare the strength of spatial autocorrelations. Cambardella et al. (1994) suggested using the ratio of the nugget-to-sill-variance for this purpose, and this approach has been widely adopted. If this ratio is $\leq 25\%$, then the variable is considered to be strongly spatially dependent; a ratio of 25–75% indicates moderate dependence, and one of 75% and more suggests weak spatial autocorrelations. In an earlier study (Zimmermann et al., 2008), we proposed to fix the nugget to the semivariance at the smallest lag since estimating the nugget variance has to be done by model extrapolation, which may obscure the inter-site comparison of the autocorrelation strength. We therefore regarded the nugget variance as fixed, i.e. it corresponds to the semivariance calculated with the above-mentioned formula of Matheron (1962) at our smallest possible lag distance of 0.25 m; for the 50 cm depth we averaged the semivariance over the first meter due to insufficient point pairs at the first lag.

In addition to the variogram analysis, we adopted an approach proposed by Bjørnstad and Falck (2001) that uses a non-parametric estimator (i.e. no a priori assumption of a functional form, e.g. Gaussian, exponential) of the covariance function, the spline correlogram, which is a generalization of the spatial correlogram. Bjørnstad and Falck (2001) applied the Fourier filter method (Hall et al., 1994) to ensure positive semidefiniteness. The assumptions which have been satisfied when using spline correlograms are the same that we checked in the course of our analysis, i.e. second-order stationarity, isotropy, and a Gaussian data distribution. The advantage of this method is the possibility to generate a confidence envelope for the covariance function by means of a bootstrap procedure. The correlation length is defined as the distance at which the covariance is not significantly different from 0; non-random local structures are indicated if the spatial autocorrelation at a separation distance of 0 (the y-intercept) is significantly positive.

Results

Exploratory data analysis

Box–Cox transformation of the global comparison datasets showed that taking logarithms would be the most appropriate transformation in the majority of the cases. There were, however, some exceptions, where the ladder of powers indicated square root transformation (pine plantation and forest at 12.5 cm depth), or transformation by the reciprocal of the square root (young fallow at 12.5 and 20 cm depth), respectively. Since it is impossible to compare differently transformed data, we used the untransformed data for the global comparisons, which reveal a high coefficient of skew in their univariate distribution (Table 2).

The spatial datasets had to be log-transformed except for the young fallow at 12.5 and 20 cm depth, where we used the reciprocal of the square root for transformation. A Gaussian distribution could be achieved for half of the datasets, whereas for the others the distributions were still somewhat skewed (Table 3).

At 12.5 cm depth, bivariate distributions as indicated by the h-scattergrams appear approximately Gaussian; i.e. the point cloud is not distorted; outlying values are also

Table 3 Distribution of the transformed spatial K_s data

Cover type	Soil depth (cm)	Skewness	p -Value ^a (Shapiro)
Pasture	12.5	0.35	0.22
	20.0	0.75	0.0001
	50.0	0.59	0.0001
Young fallow	12.5	0.74	0.0005
	20.0	0.52	0.0003
	50.0	0.04	0.51
Old fallow	12.5	0.09	0.58
	20.0	0.21	0.21
	50.0	0.73	0.001
Old landslide	12.5	−0.04	0.02
	20.0	0.08	0.13
	50.0	0.45	0.12
Natural forest	12.5	−0.39	0.005
	20.0	−0.14	0.42
	50.0	0.05	0.89

^a p -Value of the Shapiro–Wilk normality test (Shapiro and Wilk, 1965).

Table 2 Summary statistics of the K_s -data used for the global comparisons

Cover	Depth (cm)	Mean (mm/h)	LCL ^a (mm/h)	Median (mm/h)	UCL ^b (mm/h)	Skewness
Natural forest	12.5	135	−32	25	81	2.17
	20	92	5	22	39	2.48
	50	11	0	3	5	4.19
Young landslide	12.5	53	−7	12	30	3.35
	20	80	−5	23	50	1.96
	50	11	5	7	10	4.20
Old landslide (slip zone)	12.5	58	10	28	46	2.80
	20	73	−1	29	59	3.42
	50	20	−8	8	24	0.98
Pasture	12.5	14	−2	3	9	3.04
	20	17	1	2	4	3.55
	50	130	−11	11	32	2.21
Young fallow	12.5	7	1	1	2	5.04
	20	10	0	1	2	3.38
	50	10	0	1	2	5.23
Old fallow	12.5	82	0	7	15	3.00
	20	29	0	6	11	3.20
	50	12	0	2	5	5.22
Pine plantation	12.5	514	217	429	641	0.62
	20	125	6	50	94	2.38
	50	12	1	3	5	4.24
Forest	12.5	738	169	479	789	1.53
	20	130	−1	55	110	2.08
	50	178	−36	7	51	3.02

^a Lower confidence limit of the median.

^b Upper confidence limit of the median.

not highlighted (Fig. 5). The same applies to the 20 and 50 cm depth, except that the pasture has some extreme values (Figs. 6 and 7).

Significant linear trends characterize the log-transformed spatial data of the old fallow and the natural forest at all investigated soil depths (not shown). These local trends may partly be explained by the topography of those plots, e.g. the left side of the old fallow plot sloped toward a small stream, whereas its right side comprised a ridge. They may also be the consequence of too small an extent (Skøien and Bloesch, 2006). Transformed K_s of the young

fallow at 12.5 cm depth also shows a slight but significant linear trend. In any case, the location dependence of K_s may compromise the inter-site comparisons, and they have to be interpreted with caution.

Global comparisons

Depth gradient

K_s decreases with increasing depth under forest and on the old landslide (Table 2 and Fig. 8). On the young landslide, K_s is somewhat higher at 20 cm compared to 12.5 cm soil

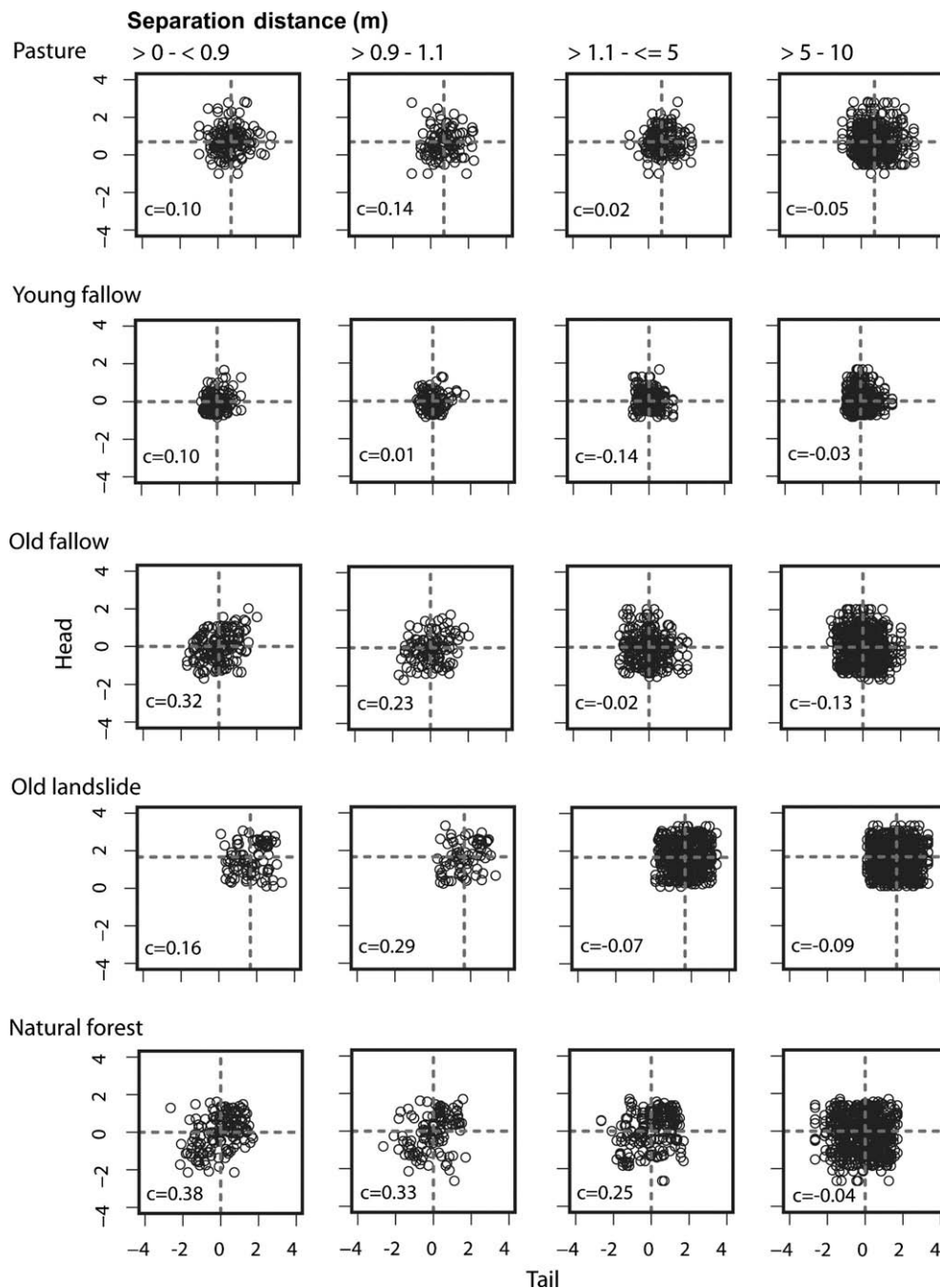


Figure 5 Bivariate distributions of the data or the residuals for the 12.5 cm soil depth; c is the Spearman rank correlation coefficient.

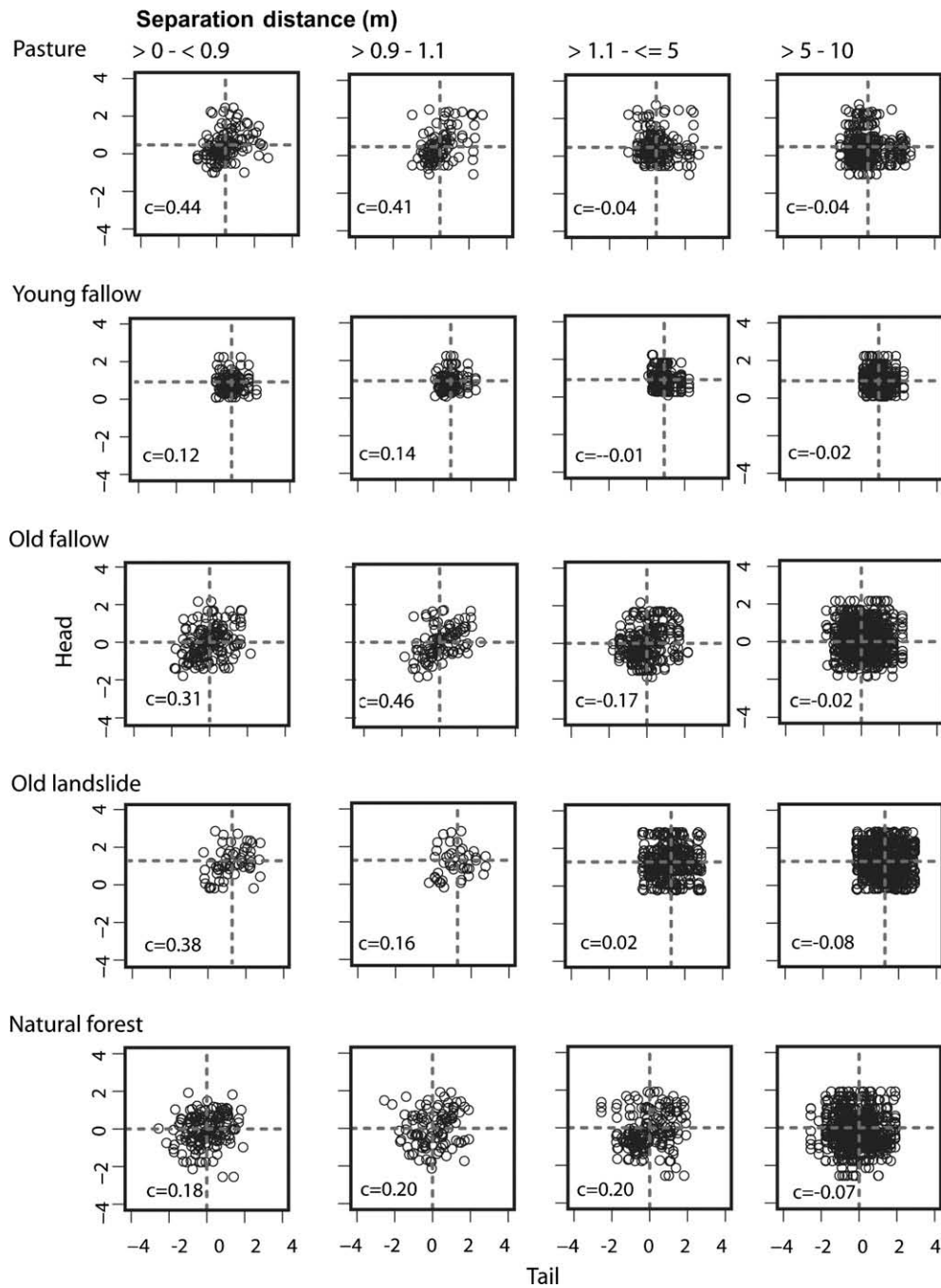


Figure 6 Bivariate distributions of the data or the residuals for the 20 cm soil depth; c is the Spearman rank correlation coefficient.

depth, but also lowest at 50 cm depth (Table 2). In all cases, the decreasing trend is, however, not significant.

At the human-influenced valley side, the drop of K_s with depth similarly occurs with the exception of pasture; here, K_s is highest at 50 cm soil depth (Table 2). Permeability under the young fallow decreases only very slightly between the topsoil and 50 cm depth. A somewhat more pronounced, but still insignificant drop characterizes K_s under the old fallow. In contrast, permeability of the soils under the pine plantation and the forest shows a significant depth gradient as it decreases by two orders of magnitude between the topsoil and 50 cm soil depth.

Inter-site comparison

The inter-site comparison for the natural disturbance sequence (Table 2) does not reveal significant changes of K_s along the pathway of recovery at any depth. Likewise the two different zones of a landslide slip zone and non-active zone do not differ significantly with respect to K_s at any depth (Fig. 8).

Human disturbance affects K_s quite differently. The two forest types do not differ significantly at any depth, but their K_s exceeds that of the pasture and the recovery stages by two orders of magnitude at the depths of 12.5 and 20 cm, respectively (Table 2). That is to say, 10 years of non-grazing

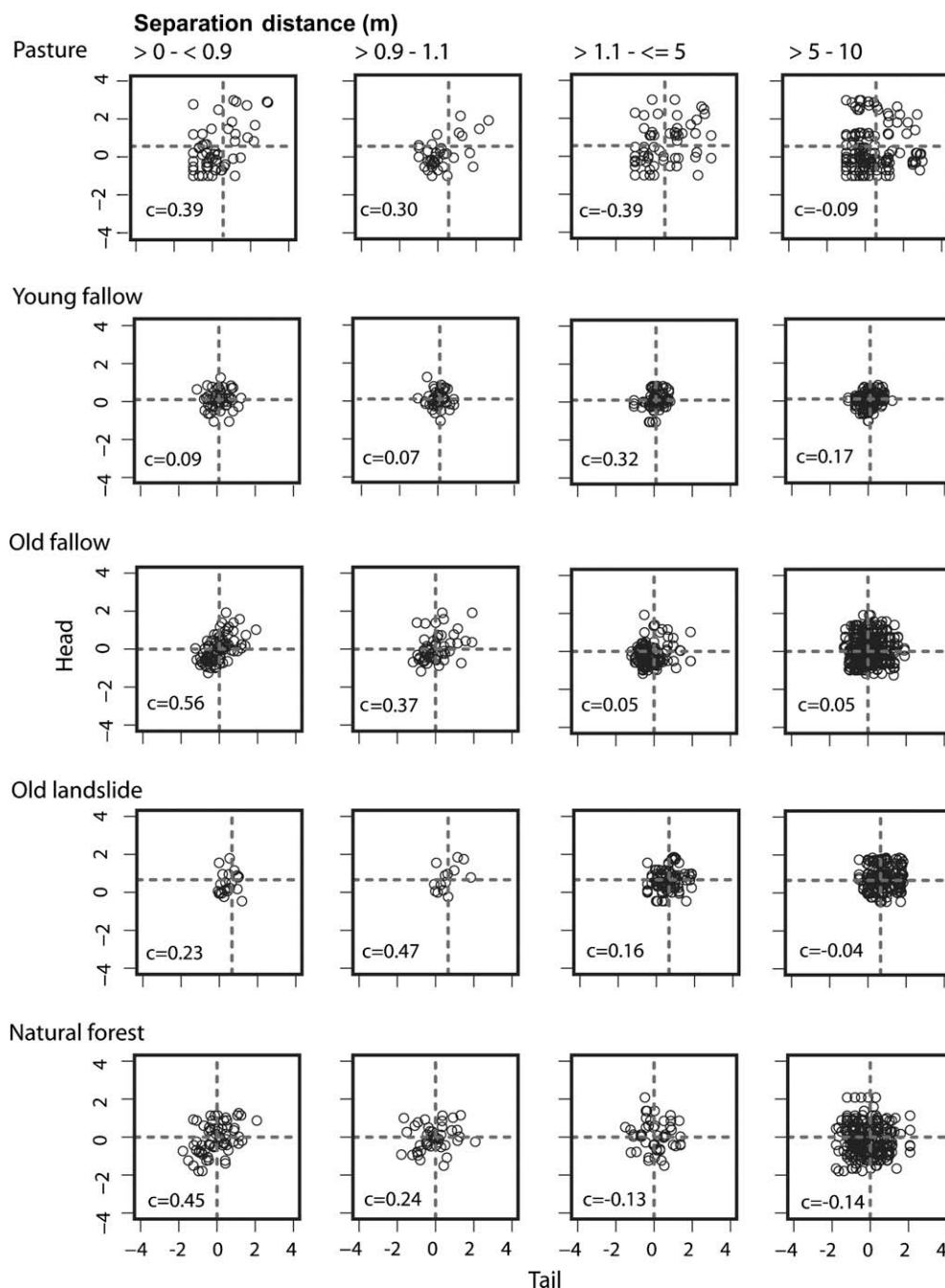


Figure 7 Bivariate distributions of the data or the residuals for the 50 cm soil depth; c is the Spearman rank correlation coefficient.

and secondary succession have yet to produce a significant increase in K_s at the depths most affected by grazing. Permeability at 50 cm depth does not differ among land covers.

Spatial variability

Robust estimation requirements and anisotropic variation

Although the univariate distribution is Gaussian for only half of the spatial datasets, the median of the θ statistics remains always within its confidence limits. These amount

to 0.286 and 0.624, respectively, for a sample size of 150, and are somewhat wider for the partly smaller sample sizes at the 50 cm soil depth. Thus, we do not need robust estimation.

There were only negligible differences in the sill variance between the least-squares models fitted to the experimental variogram and the restricted maximum likelihood estimates. We found partly greater differences between the models regarding the range, which is a result of the dependence of the least-squares model on the lag classes used for the experimental variogram (Zimmermann et al., 2008).

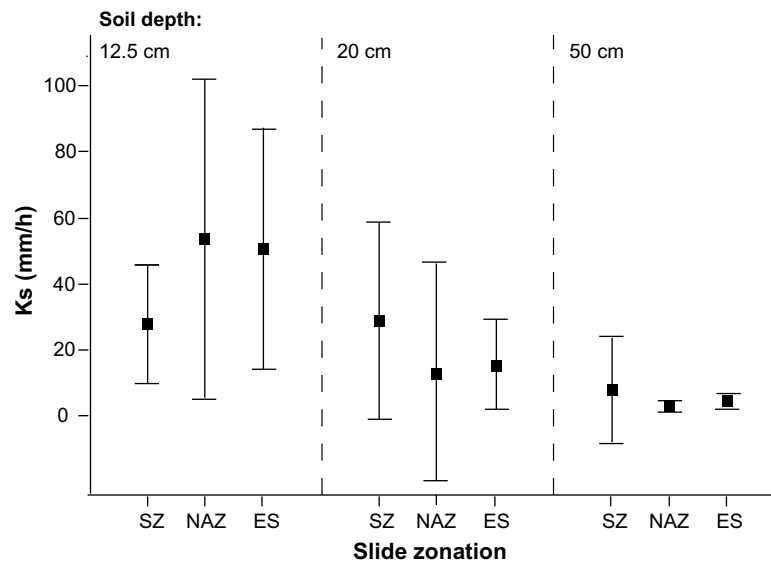


Figure 8 Median K_s under different zones on old landslide. SZ is the slip zone, NAZ the non-active zone, and ES the entire landslide. The square represents the median, and the bars below and above the median show the calculated 95% lower and upper confidence limits for the median, respectively.

In summary, we decided to use REML for the estimation of the covariance parameters for all land covers and soil depths based on the h -scattergrams and the θ statistics.

Plots of the experimental variograms in four different directions of the transformed data or the residuals of the regression, respectively, did not indicate anisotropic variation.

Depth gradient of spatial patterns

An increase of both the strength of the autocorrelation and the correlation length characterizes a number of land covers. Under pasture, the effective range increases by one order of magnitude between 12.5 and 20 and 50 cm depth, respectively (Table 4). This trend is confirmed by the spline correlograms (Fig. 9), which in addition indicate non-significant autocorrelation of the pasture topsoil permeability. The strength of the correlation similarly increases with depth under this land cover by about 20% (Table 4). A similar pattern characterizes the spatial depth gradient for the old fallow, though the effective range is shorter at 50 than at 20 cm soil depth (Table 4); it is the only land cover with significant autocorrelations at all soil depths (Fig. 9). K_s under the young fallow exhibits only a weak spatial dependence in the topsoil, and complete spatial randomness in the subsoil.

The old landslide also shows a depth-related pattern with a longer K_s correlation length in the subsoil (Table 4 and Fig. 9). Spatial correlations for K_s under the natural forest are only significant in the topsoil (Fig. 9), but apart from this no clear depth-dependent pattern emerges (Table 4).

In summary, more or less pronounced and disparate spatial depth gradients characterize the permeability of all land covers.

Spatial structure as a function of land use

In the topsoil, h -scattergrams (Fig. 5) suggest similar weak spatial autocorrelations under pasture and the young fallow with a somewhat longer correlation length for the latter cover, whereas a stronger K_s spatial dependence is indi-

cated for the old fallow. K_s of the natural forest topsoil shows both stronger and further-reaching autocorrelations compared to the landslide. The spline correlograms consistently indicate that only the old fallow and the natural forest exhibit significant K_s spatial autocorrelations, i.e. no spatial randomness (Fig. 9). This coincides with the longer effective ranges of those land covers (Table 4). The nugget-to-sill ratios indicate, however, only moderate spatial dependence regardless of land cover.

At the 20 cm depth, permeability under pasture is stronger auto-correlated at the smallest separation distance than under either fallow, but the old fallow has again the longest correlation length (Fig. 6). The K_s autocorrelation strength is similar for the forest and the landslide soil (Fig. 6). The spline correlograms (Fig. 9) indicate significant autocorrelation for pasture and the old fallow, but not for the other land covers. Although the longest effective range is associated with the young fallow (Table 4), this land cover has only a weak spatial structure compared to the other land covers, which at least show a moderate spatial dependence.

At 50 cm soil depth, complete spatial randomness characterizes the young fallow's permeability as indicated by both the spline correlograms and the variogram model. As at 20 cm depth, the spline correlograms (Fig. 9) suggest significant autocorrelations only for pasture and the old fallow; pasture K_s has the longest effective range of all land covers. The forest-landslide comparison reveals a longer effective range of the landslide K_s (Table 4), but spatial autocorrelations of both the covers are not significant as indicated by the spline correlograms (Fig. 9).

Discussion

Global comparisons

The trend of decreasing K_s with increasing depth documented for all land covers except pasture resembles that

Table 4 Summary of the REML models

Cover type	Soil depth (cm)	Model ^a	Nugget	Partial sill ^b	Sill	Range (m)	Effective range (m) ^c	Nugget/sill	Median of $\theta(x)$ ^d	Mean of $\theta(x)$ ^e	Trend coefficients		
											β_0	β_1	β_2
Pasture	12.5	Gau	0.35	0.21	0.56	0.44	0.76	0.62	0.327	0.970			
Young fallow		Gau	0.15	0.05	0.20	0.88	1.53	0.73	0.468	1.026	1.1343	-0.0063	-0.0035
Old fallow		Exp	0.39	0.22	0.61	1.15	3.46	0.64	0.437	0.929	2.4396	-0.042	-0.0021
Old landslide		Sph	0.40	0.21	0.61	4.95	4.95	0.66	0.509	0.994			
Natural forest		Sph	0.55	0.38	0.93	7.79	7.79	0.59	0.321	1.006	1.1854	-0.0067	0.0155
Pasture	20	Gau	0.42	0.17	0.59	2.38	4.12	0.71	0.215 ^f	0.972			
Young fallow		Gau	0.19	0.04	0.23	8.77	15.18	0.82	0.456	1.032			
Old fallow		Gau	0.50	0.28	0.78	4.88	8.45	0.64	0.443	0.882	2.3733	-0.0411	-0.0104
Old landslide		Sph	0.48	0.16	0.64	5.40	5.40	0.75	0.399	0.975			
Natural forest		Exp	0.59	0.21	0.80	3.39	10.18	0.74	0.557	1.086	1.1789	-0.0085	0.0088
Pasture	50	Sph	0.61	0.85	1.46	18.11	18.11	0.42	0.384	1.112			
Young fallow		Nug	0.19	0.00	0.19	0.00	0.00	1.00	0.378	1.000			
Old fallow		Gau	0.20	0.31	0.51	1.99	3.45	0.39	0.437	0.938	1.0689	-0.0028	-0.0165
Old landslide		Sph	0.20	0.13	0.33	13.69	13.69	0.60	0.304	1.041			
Natural forest		Sph	0.41	0.30	0.71	4.94	4.94	0.58	0.428	1.045	0.262	-0.0067	0.0101

^a Correlation function: Sph: spherical; Exp: exponential; Gau: Gaussian; and Nug: pure nugget.

^b Sill variance less the nugget variance.

^c For exponential model: range * 3; for Gaussian model: range * 3^{0.5}.

^d Median of the θ statistic; values outside the confidence limits are in italics.

^e Mean of the θ statistic.

^f Within confidence limits when nugget is not fixed.

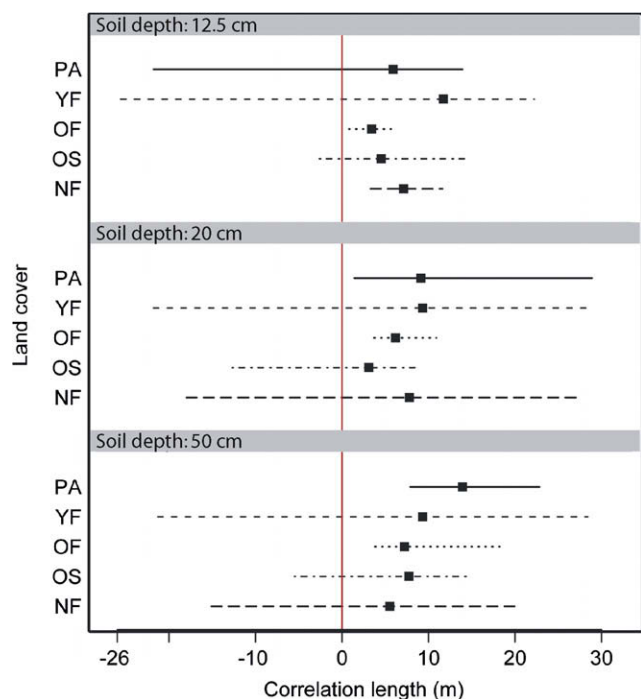


Figure 9 Correlation length estimated by the spline correlograms for the land covers pasture (PA), young fallow (YF), old fallow (OF), pine plantation (PI), and natural forest (NF). The square represents the estimate of the distance at which the similarity of two K_s values is not different of that expected by chance alone within the sample. The bars span the 95% confidence intervals, which were estimated using bootstrapping based on 1000 bootstrap samples.

found for various soil types in many humid tropical regions (e.g. Malmer, 1996, Noguchi et al., 2003). Depending on the precipitation characteristics, the hydraulic discontinuity with depth may be significant for shallow landslide initiation (Sidle and Ochiai, 2006). Vieira and Fernandes (2004), for instance, found a decrease by two orders of magnitude between the depths of 0.30 and 0.60 m for a number of profiles close to the border and inside landslide scars in Rio de Janeiro.

The increase of K_s with depth under pasture was an exceptional case within the disturbance-recovery sequences. Several explanations might be proposed for this soil hydraulic behavior (e.g. high porosity in weathered sandstones; steeply inclined stone layers); the inter-site comparison, however, was not influenced in terms of a significant difference at the 50 cm soil depth.

The remarkable lower surface soil permeability of pasture and the two fallow systems compared to the pine plantation and forest emphasizes the critical influence of land cover change on soil hydrology. At the 50 cm depth, the disappearance of land use effects on K_s matches observations from lowland Amazonia (Zimmermann et al., 2006), where K_s was independent of land cover at a depth of only 20 cm.

Within the humid tropics, the impact of forest conversion or disturbance for timber harvesting or agricultural use on infiltrability has been shown in a number of studies (e.g. Malmer, 1996; Hanson et al., 2004). Ziegler et al. (2004) de-

scribed the behavior of K_s in a land use sequence including upland fields, fallows and secondary forests in mountainous Vietnam, and reported a decline of K_s under the disturbed land covers compared to a reference forest as well as a regeneration of soil permeability some years after land use abandonment. Alegre and Cassel (1996) and Martinez and Zinck (2004) found a decline of infiltrability after pasture establishment for an Ultisol in Peru and Colombia, respectively.

Lal (1996), working in western Nigeria, reported a decreased permeability under pasture, similar to that reported for Amazonia (Tomasella and Hodnett, 1996; Zimmermann et al., 2006). In a temperate rainforest region, McDowell et al. (2003) showed that simulated cattle treading indeed caused a decrease in surface permeability. Consequently, we also attribute the reduced permeability under the Ecuadorian pasture to the effect of soil compaction caused by cattle treading.

A recovery of K_s after pasture abandonment was observed in Amazonia (Godsey and Elsenbeer, 2002; Zimmermann et al., 2006). Comparing our results with the above – mentioned lowland rainforest studies, it turns out that the decline of near – surface K_s after pasture establishment occurs in lowland as well as in upland tropical regions. The recovery process is still insufficiently understood for general statements; the results from Amazonia and the montane rainforest in Ecuador, however, suggest that the deterioration of soil permeability under pasture is reversible after some time following abandonment.

In Ecuador, we estimate this recovery time of surface K_s to exceed a decade since permeability under the old fallow still resembles that of the pasture. After a quarter of a century, the former land use signal is likely to vanish, if the recovery documented for the pine plantation (Table 2) is any indication.

In order to explain the uniform permeability under the slides and the forest in the topsoil, we propose that landslides in the study region basically remove the biomass and the organic layer, but only a thin topsoil layer; thus, their impact on the mineral soil, and hence its K_s , is marginal. The soil hydraulic similarity of soil removal and accumulation zones of the old landslide and the rareness of actual landslides in the cleared areas also supports this hypothesis. Nonetheless, ours shares the limitation of any case study in that its regional representativeness is difficult, if not impossible, to assess in any quantitative sense.

Our results accord with Wilcke et al. (2003), who investigated soils under landslides in our study area, including the old landslide. They concluded that the removal of the organic layer due to landslides is the most obvious change in soil properties regarding soil morphology and nutrient concentrations. Hou et al. (2005), working in a subtropical lowland forest, found in a study of litter decomposition by soil animals under undisturbed forest and recent landslide-disturbed sites that soil fauna recovers in very short periods of time after landslide disturbance. In our study region, soil macrofauna is not abundant (Maraun et al., 2008); hence, only few macropores originate from animal activity. In this context, we found only very few visible macropores in soil clods and profile faces in the forest plot. Vieira and Fernandes (2004) investigated landslide scars along the Papagaio basin near Rio de Janeiro, where they measured K_s at four

slope positions on and next to the scars. At 30 and 60 cm soil depth, K_s hardly differed among those positions. This similarity of K_s between the upper soil layers of landslides and undisturbed areas is consistent with our observations.

Spatial variability

The spatial depth gradients highlight some special cases within the human disturbance-recovery cycle, which were also evident in the global comparisons. In the case of pasture, the high subsoil K_s coincides with a more pronounced spatial structure at 50 cm depth compared to the near-surface soil. That is to say, the unknown process which caused a number of unusual high permeability values is associated with a spatially dependent random variation. The young fallow is also exceptional in that the very low permeability throughout the investigated depth range is associated with a very weak or inexistent spatial structure. In summary, we have to state that there is no generalizable depth-related spatial pattern: some land covers have a stronger K_s spatial dependence in the subsoil (pasture, old fallow), some are rather depth-independent (old landslide, natural forest), and the young fallow K_s exhibits spatial randomness in the subsoil. Hence, the evident depth gradient of average K_s has no analog in its spatial structure; e.g. lower subsoil permeability might on the one hand coincide with a more pronounced spatial dependence (e.g. old fallow), and can on the other hand be associated with a spatial pattern similar to the near-surface soil (i.e. natural forest). These variations in spatial depth gradients are reflected in the literature about K_s spatial variability of agricultural land.

Mallants et al. (1996) reported a decrease of spatial dependence with increasing depth; Mohanty and Mousli (2000) found a decrease of correlation length, but increase of the correlation strength between 15 and 30 cm soil depth; Iqbal et al. (2005) also reported an increase of the correlation length moving from the surface to the deeper soil.

Some similarities characterize the spatial inter-site comparisons. First, the nugget-to-sill ratios indicate moderate spatial dependence in the topsoil; i.e. the partial sill contributes to about 30–40% to the total sill, which is therefore dominated by the nugget variance (Table 4). The high contribution of the nugget can be caused by high measurement errors (which we cannot quantify) or by a very small-scale variability. Since the measurement error should not vary much among the land covers, the small-scale variability seems to be of similar quantity for all of them. Some land use related pattern regarding the strength of the spatial autocorrelation are indicated by the h-scattergrams for the topsoil (Fig. 5), as the correlation is stronger for point pairs of the old fallow and forest K_s separated by small distances. Those differences, however, are not reflected in the variogram model one would use for spatial prediction (the sill variance is certainly somewhat biased due to departures from the Gaussian distribution for pasture and young fallow, but the models are adequate for kriging). Hence, from a practical point of view, the strength of K_s spatial dependence appears to be independent of land cover. In contrast, the correlation length seems to be a function of disturbance as the less disturbed soils of the old fallow and the natural forest have longer effective ranges than their disturbed counterparts. These land cover-related differences

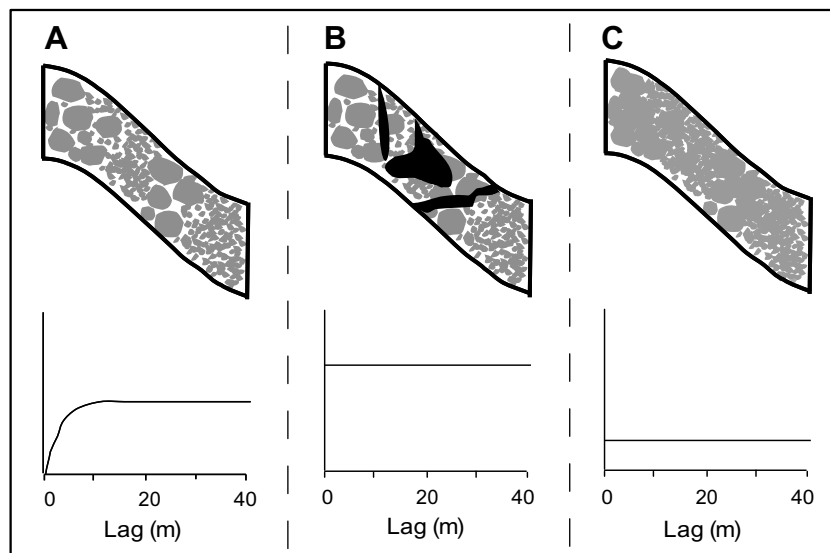


Figure 10 Possible effect of soil disturbances on K_s spatial structure. (A) Soil column with intrinsic textural variation with alternating zones of high (where texture is coarse) and low (where texture is fine) K_s , and the corresponding variogram. Spatially dependent random variation in permeability can also be caused by intrinsic or extrinsic variations in soil structure, e.g. as a function of vegetation cover. (B) The same soil column with biogenetic macropores (black entities), and the corresponding variogram. The spatially dependent random variation disappears or is very small-scale, which generates a flat or a pure-nugget variogram with a greater sill variance than that of A. Other examples of group B include soil cracks caused by freezing and thawing cycles. (C) The same soil column which has undergone a compaction, e.g. by cattle treading. Permeabilities are generally low. The corresponding variograms tend to pure nugget solely comprising the random error; the sill variance is smaller compared to the variogram of A. Tillage operations are likely to have the same effect.

influence the spatial prediction; that is to say, exercises which require interpolated permeabilities, e.g. as an input in hydrological models, have to take into account the land-use effect.

The greatest variations in both the range and the strength of spatial autocorrelations are found at the depth of 50 cm (Table 4). The partial sill contributes between 0% (young fallow) and 60% (old fallow) to the total sill variance, and the effective ranges encompasses 0 (young fallow) to 20 m (pasture). As for average K_s values, land use is not an influential factor in the subsoil. But in contrast to simple location estimates, which at least do not differ significantly among the land covers, the covariance parameters are site-specific. That is to say, spatial interpolation is even more complicated than for the topsoil, where land use may be a proxy for the development of a predictable spatial structure. Hence, spatial interpolation is certainly inaccurate when taking the covariance parameters of maybe similar but not identical sites from the literature. This site dependence of the covariance function adds to the fact that in the present as well as in the bulk of similar studies the local and not the theoretical variogram is estimated, as the accuracy of the latter depends on the sample scale triplet relative to the (mostly unknown) scales of the underlying process (Bloeschl and Sivapalan, 1995; Skøien and Bloeschl, 2006).

Inter-site comparisons of the K_s spatial structure are lacking in the literature. There are some indications, however, that a predictable spatial structure might be associated with stable soil conditions (Reynolds and Zebchuk, 1996; Mohanty and Mousli, 2000; ?). In contrast, a spatially independent random variation seems to originate from processes that interrupt the spatially-dependent intrinsic variations as e.g. biogenic macroporosity (Sobieraj et al., 2004), uneven breaking of soil structure due to freezing and thawing (Mohanty et al., 1991), or surface tillage in the upper horizons (Bosch and West, 1998). Our results for the topsoil spatial structure suggest that the impact of cattle treading and land-sliding might integrate into such processes. Fig. 10 provides a conceptual framework, which proposes that even though the causes of disturbances are contrary (creation versus damage of macropores) their effect on the K_s spatial structure is similar, i.e. a loss of a spatially dependent random variation.

Conclusions

We answer the research questions posed in the introduction as follows:

- (1) The soil hydraulic responses to disturbance and recovery are completely different for natural and man-made disturbance regimes in this tropical montane forest. The saturated hydraulic conductivity of the two investigated landslides is undistinguishable from the reference state. We therefore assume that landslides in our study area affect mainly organic horizons, but not the mineral soil. In contrast, forest conversion to pasture and subsequent grazing are accompanied by a reduction of surface K_s of two orders of magnitude, which we attribute to soil compaction due to cattle treading.
- (2) The reduction of the permeability under cattle pasture is reversible, but the recovery after pasture abandonment likely requires at least one decade.
- (3) Disturbance and recovery effects on K_s spatial structure are evident in the topsoil of the natural forest and the old fallow, which exhibit significant autocorrelations. However, greatest variations in the covariance parameters between the land covers are found in the subsoil, where the correlation length varies between 0 and 20 m, and the portion of the nugget encompasses 30–100% of the total sill variance. These differences are site-specific and cannot be explained by disturbance.

In summary, this case study suggests a rather disparate soil hydraulic response to regionally important disturbances as cattle grazing strongly affects the spatial mean of K_s , whereas landslides don't, and both processes affect the spatial structure of K_s in the topsoil. Consequently, practical applications requiring K_s input data, e.g. hydrological models, need to incorporate the land-use effect on average values. Spatial interpolation can only be done site-specific, and any spatial mapping would require a high sample size due to rather short-range autocorrelations.

Acknowledgements

We thank the German Research Foundation (DFG) for funding the project (FOR 402, TP B3, El 255/4-1), the Fundación San Francisco (Nature and Culture International (NCI)) for providing the study area and the research station, our field assistants, and B. Huwe, F. Makeschin, and W. Wilcke for providing soil texture data. This paper benefited from the critical comments of the associate editor and two anonymous reviewers.

References

- Ahuja, L.R., Naney, J.W., Gree, R.E., Nielsen, D.R., 1984. Macroporosity to characterize spatial variability of hydraulic conductivity and effects of land management. *Soil Sci. Soc. Am. J.* 48, 699–702.
- Alegre, J.C., Cassel, D.K., 1996. Dynamics of soil physical properties under alternative systems to slash-and-burn. *Agric. Ecosyst. Environ.* 58, 39–48.
- Amoozegar, A., 1989a. A compact, constant-head permeameter for measuring saturated hydraulic conductivity of the vadose zone. *Soil Sci. Soc. Am. J.* 53, 1356–1361.
- Amoozegar, A., 1989b. Comparison of the Glover solution with the simultaneous-equations approach for measuring hydraulic conductivity. *Soil Sci. Soc. Am. J.* 53, 1362–1367.
- Amoozegar, A., 1993. Comments on "Methods for analyzing constant-head well permeameter data". *Soil Sci. Soc. Am. J.* 57, 559–560.
- Bjørnstad, O.M., Falck, W., 2001. Nonparametric spatial covariance functions: estimation and testing. *Environ. Ecol. Stat.* 8, 53–70.
- Bloeschl, G., Sivapalan, M., 1995. Scale issues in hydrological modelling – a review. *Hydrol. Proc.* 9, 251–290.
- Bosch, D.D., West, L.T., 1998. Hydraulic conductivity variability for two sandy soils. *Soil Sci. Am. J.* 62, 90–98.
- Box, G.E.P., Cox, D.R., 1964. An analysis of transformations. *J. Royal Stat. Soc., Ser. B* 26, 211–246.

- Brenning, A., 2005. Spatial prediction models for landslide hazards: review, comparison and evaluation. *Natural Hazards Earth Syst. Sci.* 5, 853–862.
- Bruijnzeel, L.A., 2001. Hydrology of tropical montane cloud forests: a reassessment. *Land Use Water Resour. Res.* 1, 1–18.
- Bruijnzeel, L.A., Hamilton, L.S., 2000. Up in the clouds. Decision time for cloud forests IHP Humid Tropics Programme Series, vol. 13. IHP-UNESCO, Paris.
- Cambardella, C.A., Moorman, T.B., Novak, J.M., Parkin, T.B., Karlen, D.L., Turco, R.F., Konopka, A.E., 1994. Field-scale variability of soil properties in central Iowa soils. *Soil Sci. Soc. Am. J.* 58, 1501–1511.
- Carman, P.C., 1956. *Flow of Gases Through Porous Media*. Academic Press, New York.
- Erick, D.E., Reynolds, W.D., 1992. Methods for analyzing constant-head well permeameter data. *Soil Sci. Soc. Am. J.* 56, 320–323.
- Fisher, R.A., 1972. *Statistical Methods for Research Workers*. Oliver & Boyd, Edinburgh.
- Godsey, S., Elsenbeer, H., 2002. The soil hydrologic response to forest regrowth: a case study from southwestern Amazonia. *Hydrol. Process.* 16, 1519–1522.
- Goller, R., Wilcke, W., Leng, M.J., Tobschall, H.J., Wagner, K., Valarezo, C., Zech, W., 2005. Tracing water paths through small catchments under a tropical montane rain forest in south Ecuador by an oxygen isotope approach. *J. Hydrol.* 308, 67–80.
- Guenter, S., Weber, M., Erreis, R., Aguirre, N., 2006. Influence of distance to forest edges on natural regeneration of abandoned pastures: a case study in the tropical mountain rain forest of Southern Ecuador. *Eur. J. Forest Res.* doi:10.1007/s10342-006-0156-0.
- Hall, P., Fisher, N.I., Hoffmann, B., 1994. On the nonparametric estimation of covariance functions. *Ann. Stat.* 22, 2115–2134.
- Hanson, D.L., Steenhuis, T.S., Walter, M.F., Boll, J., 2004. Effects of soil degradation and management practices on the surface water dynamics in the Talgua River Watershed in Honduras. *Land Degrad. Develop.* 15, 367–381.
- Hartig, K., Beck, E., 2003. The bracken fern (*Pteridium aquilinum*) dilemma in the Andes of South Ecuador. *Ecotropica* 9, 3–13.
- Hou, P.C.L., Zou, X.M., Huang, C.Y., Chien, H.J., 2005. Plant litter decomposition influenced by soil animals and disturbance in a subtropical rainforest of Taiwan. *Pedobiologia* 49, 539–547.
- Huwe, B., Zimmermann, B., Zeilinger, J., Quizhpe, M., Elsenbeer, H., 2008. Gradients and patterns of soil physical parameters at local, field and catchment scales. In: Beck, E., Bendix, J., Kottke, I., Makeschin, F., Mosandl, R. (Eds.), *Gradients in a Tropical Mountain Ecosystem of Ecuador*, Ecological Studies, vol. 198, Springer-Verlag.
- Iglewicz, B., 1983. Robust scale estimators and confidence intervals for location. In: Hoaglin, D.C., Mosteller, F., Tukey, J.W. (Eds.), *Understanding Robust and Exploratory Data Analysis*. Wiley, New York, pp. 404–429.
- Iqbal, J., Thomasson, J.A., Jenkins, J.N., Owens, P.R., Whisler, F.D., 2005. Spatial variability analysis of soil physical properties of alluvial soils. *Soil Sci. Soc. Am. J.* 69, 1338–1350.
- Lal, R., 1996. Deforestation and land-use effects on soil degradation and rehabilitation in western Nigeria. 1. Soil physical and hydrological properties. *Land Degrad. Develop.* 7, 19–45.
- Lark, R.M., 2000. A comparison of some robust estimators of the variogram for use in soil survey. *Eur. J. Soil Sci.* 51, 137–157.
- Lark, R.M., Cullis, B.R., Welham, S.J., 2006. On spatial prediction of soil properties in the presence of a spatial trend: the empirical best linear unbiased predictor (E BLUP) with REML. *Eur. J. Soil Sci.* 57, 787–799.
- Larsen, M.C., Torres-Sanchez, A.J., Concepcion, I.M., 1999. Slope-wash, surface runoff and fine-litter transport in forest and landslide scars in humid-tropical steepplands, Luquillo Experimental Forest, Puerto Rico. *Earth Surf. Proc. Landforms* 24, 481–502.
- Makeschin, F., Haubrich, F., Abiy, M., Burneo, J.I., Klinger, T., 2008. Pasture management and natural soil regeneration. In: Beck, E., Bendix, J., Kottke, I., Makeschin, F., Mosandl, R. (Eds.), *Gradients in a Tropical Mountain Ecosystem of Ecuador*, Ecological Studies, vol. 198, Springer-Verlag.
- Mallants, D., Mohanty, B.P., Jacques, D., Feyen, J., 1996. Spatial variability of hydraulic properties in a multi-layered soil profile. *Soil Sci.* 161, 167–181.
- Malmer, A., 1996. Hydrological effects and nutrient losses of forest plantation establishment on tropical rainforest land in Sabah, Malaysia. *J. Hydrol.* 174, 129–148.
- Maraun, M., Illig, J., Sandman, D., Krashevskaya, V., Norton, R.A., Scheu, S., 2008. Soil fauna. In: Beck, E., Bendix, J., Kottke, I., Makeschin, F., Mosandl, R. (Eds.), *Gradients in a Tropical Mountain Ecosystem of Ecuador*, Ecological Studies, vol. 198, Springer-Verlag.
- Martinez, L.J., Zinck, J.A., 2004. Temporal variation of soil compaction and deterioration of soil quality in pasture areas of Colombian Amazonia. *Soil Till. Res.* 75, 3–17.
- Matérn, B., 1960. Spatial variation. *Meddelanden fr3n Statens Skogsforskningsinstitut* 49 (5) (Lecture Notes in Statistics, second ed. vol. 36, Springer, New York, 1986).
- Matheron, G., 1962. *Traité de Géostatistique Appliqué*, Tome 1. *Memoires du Bureau de Recherches Géologiques et Minières*, Paris.
- McDowell, R.W., Drewry, J.J., Paton, R.J., Carey, P.L., Monaghan, R.M., Condron, L.M., 2003. Influence of soil treading on sediment and phosphorus losses in overland flow. *Aust. J. Soil Res.* 41, 949–961.
- Mohanty, B.P., Mousli, Z., 2000. Saturated hydraulic conductivity and soil water retention properties across a soil-slope transition. *Water Resour. Res.* 36, 3311–3324.
- Mohanty, B.P., Kanwar, R.S., Horton, R., 1991. A robust-resistant approach to interpret spatial behavior of saturated hydraulic conductivity of a glacial till soil under no-tillage system. *Water Resour. Res.* 27, 2979–2992.
- Motzer, T., Munz, N., Kuppers, M., Schmitt, D., Anhof, D., 2005. Stomatal conductance, transpiration and sap flow of tropical montane rain forest trees in the southern Ecuadorian Andes. *Tree Physiol.* 25, 1283–1293.
- Muñoz, C.J.C., 2005. Cuantificación de la variabilidad de las propiedades del suelo, a pequeña escala, utilizando métodos geostatísticos en la Estación Científica San Francisco. Diploma Thesis, Universidad Nacional de Loja, Ecuador.
- Noguchi, S., Kasran, B., Yusop, Z., Tsuboyama, Y., Tani, M., 2003. Depth and physical properties of soil in a forest and a rubber plantation in peninsular Malaysia. *J. Tropical Forest Sci.* 15, 513–530.
- Pardo-Igúzquiza, E., 1998. Maximum likelihood estimation of spatial covariance parameters. *Math. Geol.* 30, 95–108.
- Pebesma, E.J., 2004. Multivariable geostatistics in S: the gstat package. *Compos. Geosci.* 30, 683–691.
- R Development Core Team, 2004. *R: A language and environment for statistical computing*. R Foundation for Statistical Computing, Vienna, Austria.
- Reynolds, W.D., Zebchuk, W.D., 1996. Hydraulic conductivity in a clay soil: two measurement techniques and spatial characterization. *Soil Sci. Soc. Am. J.* 60, 1679–1685.
- Ribeiro, P.J., Diggle, P.J., 2001. *GeoR: a package for geostatistical analysis*. R-NEWS, vol. 1 (2) <<http://cran.r-project.org/doc/Rnews>>.
- Ringrose-Voase, A.J., 1991. Micromorphology of soil structure: description, quantification, application. *Aust. J. Soil Res.* 29, 777–813.
- Rollenbeck, R., Bendix, J., Fabian, P., Boy, J., Dalitz, H., Emck, P., Oesker, M., Wilcke, W., 2007. Comparison of different techniques for the measurement of precipitation in tropical montane rain forest regions. *J. Atmos. Ocean. Technol.* 24, 156–168.

- Schrumpf, M., Guggenberger, G., Valarezo, C., Zech, W., 2001. Tropical montane rain forest soils. Development and nutrient status along an altitudinal gradient in the south Ecuadorian Andes. *Die Erde* 132, 43–60.
- Shapiro, S.S., Wilk, M.B., 1965. An analysis of variance test for normality (complete samples). *Biometrika* 52, 591–611.
- Shukla, M.K., Slater, B.K., Lal, R., Cepuder, P., 2004. Spatial variability of soil properties and potential management classification of a chernozemic field in lower Austria. *Soil Sci.* 169, 852–860.
- Sidle, R.C., Ochiai, H., 2006. Subsurface flow processes. In: *Landslides: Processes, Prediction, and Land Use*. American Geophysical Union, Washington, DC, pp. 76–80.
- Singh, K.P., Mandal, T.N., Tripathi, S.K., 2001. Patterns of restoration of soil physicochemical properties and microbial biomass in different landslide sites in the sal forest ecosystem of Nepal Himalaya. *Ecol. Eng.* 17, 385–401.
- Skøien, J.O., Bloeschl, G., 2006. Scale effects in estimating the variogram and implications for soil hydrology. *Vadose Zone J.* 5, 153–167.
- Sobieraj, J.A., Elsenbeer, H., Cameron, G., 2004. Scale dependency in spatial patterns of saturated hydraulic conductivity. *Catena* 55, 49–77.
- Soil Survey Staff, 1999. *Soil Taxonomy – A Basic System of Soil Classification for Making and Interpreting Soil Surveys*, second ed. US Government Printing Office, Washington, DC.
- Terlien, M.T.J., 1997. Hydrological landslide triggering in ash-covered slopes of Manizales (Colombia). *Geomorphology* 20, 165–175.
- Tomasella, J., Hodnett, M.G., 1996. Soil hydraulic properties and van Genuchten parameters for an oxisol under pasture in central Amazonia. In: Gash, J.H.C., Nobre, C.A., Roberts, J.M., Victoria, R.L. (Eds.), *Amazonian Deforestation and Climate*. John Wiley & Sons, Chichester, pp. 101–124.
- Vieira, B.C., Fernandes, N.F., 2004. Landslides in Rio de Janeiro: the role played by variations in soil hydraulic conductivity. *Hydrol. Process.* 18, 791–805.
- Walker, L.R., Zarin, D.J., Fetcher, N., Myser, R.W., Johnson, A.H., 1996. Ecosystem development and plant succession on landslides in the Caribbean. *Biotropica* 28, 566–576.
- Webster, R., Oliver, M.A., 1992. Sample adequately to estimate variograms of soil properties. *J. Soil Sci.* 43, 177–192.
- Webster, R., Oliver, M.A., 2001. *Geostatistics for Environmental Scientists*. John Wiley & Sons, Chichester, UK.
- Whittle, P., 1954. On stationary processes in the plane. *Biometrika* 41, 434–449.
- Wilcke, W., Valladarez, H., Stoyan, R., Yasin, S., Valarezo, C., Zech, W., 2003. Soil properties on a chronosequence of landslides in montane rain forest, Ecuador. *Catena* 53, 79–95.
- Zaitchik, B.F., Van Es, H.M., Sullivan, P.J., 2003. Modeling slope stability in Honduras: parameter sensitivity and scale of aggregation. *Soil Sci. Soc. Am. J.* 67, 268–278.
- Ziegler, A.D., Giambelluca, T.W., Tran, L.T., Vana, T.T., Nullet, M.A., Fox, J., Vien, T.D., Pinthong, J., Maxwell, J.F., Evett, S., 2004. Hydrological consequences of landscape fragmentation in mountainous northern Vietnam: evidence of accelerated overland flow generation. *J. Hydrol.* 287, 124–146.
- Zimmermann, B., Elsenbeer, H., De Moraes, J.M., 2006. The influence of land-use changes on soil hydraulic properties: implications for runoff generation. *Forest Ecol. Manage.* 222, 29–38.
- Zimmermann, B., Zehe, E., Hartmann, N.K., Elsenbeer, H., 2008. Analyzing spatial data – an assessment of assumptions, new methods, and uncertainty using soil hydraulic data. *Water Resour. Res.*, in press. doi:10.1029/2007WR006604.